Beam Physics Note
TRI-BN-24-05
February 29, 2024

A Record of OLIS Steerer Lensing

Olivier Shelbaya, Joseph Adegun

TRIUMF

Abstract: This document records the investigation into the MCIS fringe field and its effects upon beam steering at OLIS. Evidence for lensing effects by the OLIS beamline's electrostatic steerers is presented. These are found to be prevalent both with and without the OLIS-MCIS installed in the high voltage cage.

4004 Wesbrook Mall, Vancouver, B.C. Canada V6T 2A3 · Tel: 604 222-1047 · www.triumf.ca

1 Background

Strong steering is used at OLIS, with transverse voltage difference on the order of hundreds of volts, for operation of each of the sources, to varying degrees. This report presents OLIS emittance data taken in Feb. 2024 at a relatively low energy of 8.16 keV. With an MCAT established tune for the quadrupoles, which were left untouched, the OLIS steering was altered, revealing focal effects upon the beam in the horizontal (dispersive) plane.

2 MWS Extraction System

The extraction system of the MWS was based on the H^- source developed by K. Jayamanna for the TRIUMF cyclotron [1]. Over time, several changes were made to the extraction system that were not documented[2, 3, 4]. As a result, the dimensions of the extraction aperture and extraction gap needed for source simulations in IGUN[5] cannot be determined. This makes it necessary to estimate the initial beam distribution from the ion source used in the TRANSOPTR calculation.

3 MCAT OLIS Tune

For both employed beams, the high-level application MCAT was used to compute the OLIS tune, using the sequential optimization method[6, 7]. Optimization parameters for the tune are listed in Figure 1. The envelopes for $^{40}Ar^+$ are shown in the figure, for starting beam parameters shown to the left of Figure 2.

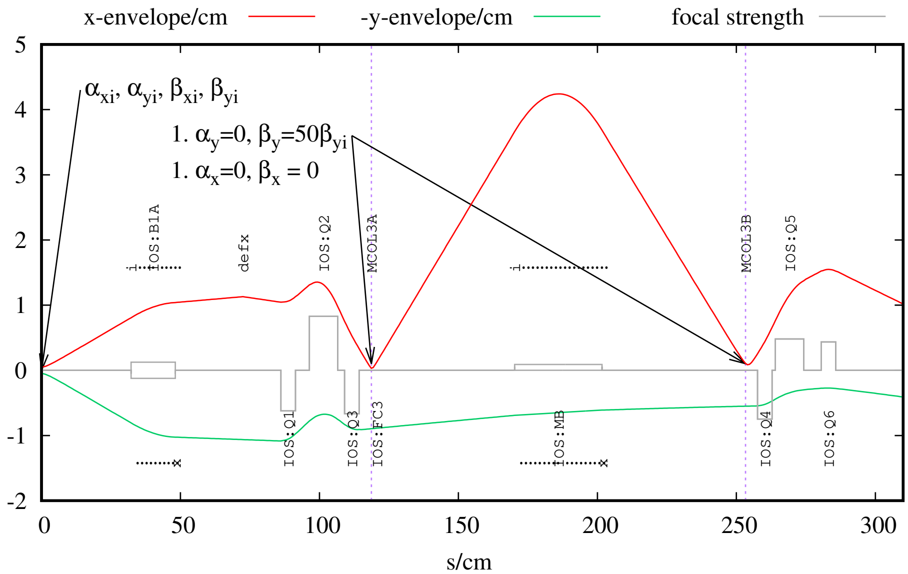

Figure 1: `MCAT` computed OLIS-MWS tune for ^{40}Ar^{+} at 8.16keV energy. Collimator fit constraints are shown on the plot, including reference to the starting beam twiss parameters at source extraction. IOS:Q4 to Q8 are tuned by MCAT, matching into the LE transport tunes. Simulation terminates at OLIS horizontal emittance rig.

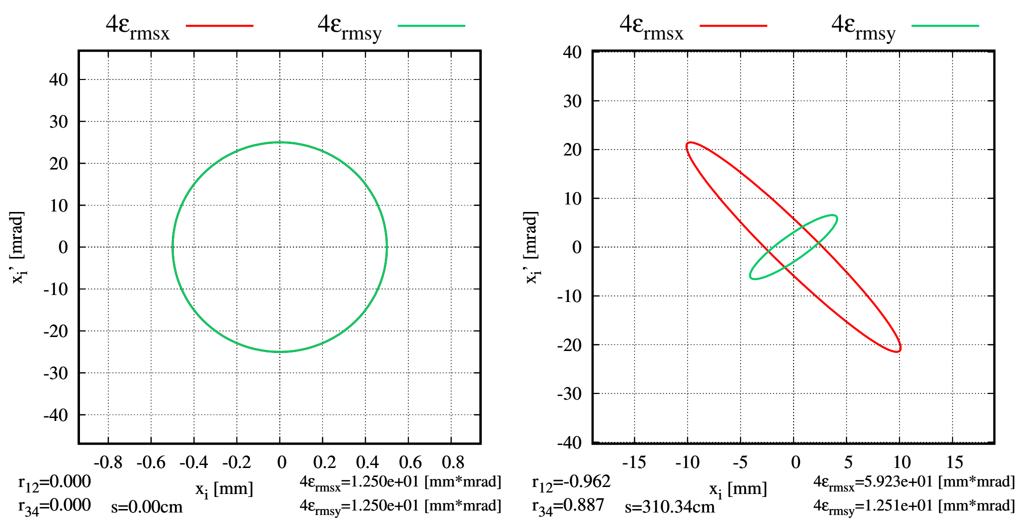

Figure 2: `TRANSOPTR` starting beam parameters (left) from MWS, and (right) at the location of the OLIS horizontal emittance rig. Note: while only the vertical distribution is visible on the left, both (x, y) distributions are identical and overlap.

Establishment of a dedicated quadrupole tune for the entirety of the OLIS tests was intended to prevent manual quadrupole optimizations, which also cause transverse beam steering. The model computed optics were loaded to the control system, necessitating only tuning of the OLIS steerers. Starting beam parameters shown in Fig. 2 were based on reasonable guesses, not on-line measurements.

3.1 On the OLIS Optics

The MCAT model for OLIS has been documented in [4]. Additionally, findings from [3] and [8] suggest longitudinal misplacement of IOS:Q2 and Q5, with possible longitudinal misplacement of MCOL3A and 3B. Spherical bender IOS:B1A remains likely in a state of misalignment, evidenced by the requirement for strong horizontal steering by IOS:XCB1, immediately downstream of MWS (or SIS) extraction.

In the following sections, each emittance scan is taken with quadrupoles at constant settings; they are not changed in any way. Only corrective steerers and common plates are tuned.

4 Notes and Findings

This section refers to OLIS horizontal emittances presented in Sections 5 and 6.

Strong steering at OLIS is required due to both misalignment of the beamline, due to factors such as the shifting of the ISAC experimental hall floor[9] and potential misalignment of the spherical bender IOS:B1A[3]. Lack of a positional diagnostic upstream of the IOS dipole[3] means no information is available regarding the beam centroid before the source faraday cup.

Note 1: Strong transverse steering is required at OLIS, both with and without the MCIS installed in the OLIS cage, from MWS and SIS extraction.

The constant requirement for strong transverse steering at OLIS causes large voltage differences on the OLIS (x, y) corrective steerers.

Note 2: Grounded skimmer electrodes for steerers possess circular apertures at ISAC.

Note 3: ISAC corrective steerer plates are held at the same polarity.

A schematic of an ISAC steerer module is shown in Fig. 3 and its field in Fig. 4. The noted conditions cause a quadrupole-like focal effect as reported in [10, 11].

Finding 1: OLIS steerers cause an energy-dependent lensing effect, which will be more pronounced at lower beam energies. This affects all OLIS beams, whether from MWS, SIS or MCIS.

Finding 2: A similar issue was previously tackled at I1 with the cyclotron injection line[11].

Finally, note that full characterization of the steerer lensing effect is beyond the scope of this report, and will be pursued in future work.

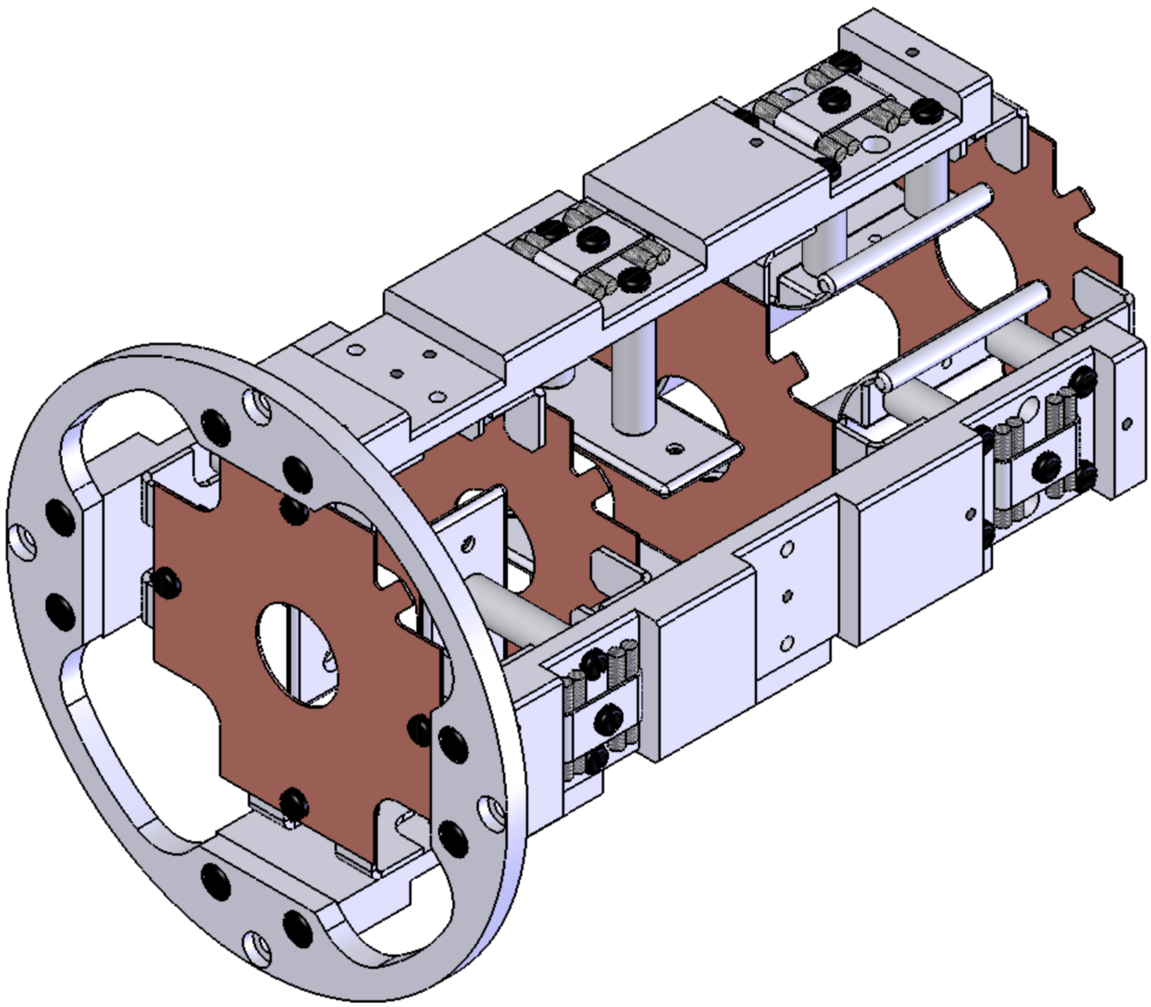

Figure 3: Schematic representation of an ISAC (x, y) electrostatic steerer assembly, obtained from drawing `ILE2116D`. Note the round skimmer apertures on the grounded skimmer plates (brown), which are perpendicular to the beam propagation axis. This particular module also contains an electrostatic quadrupole (top, right side).

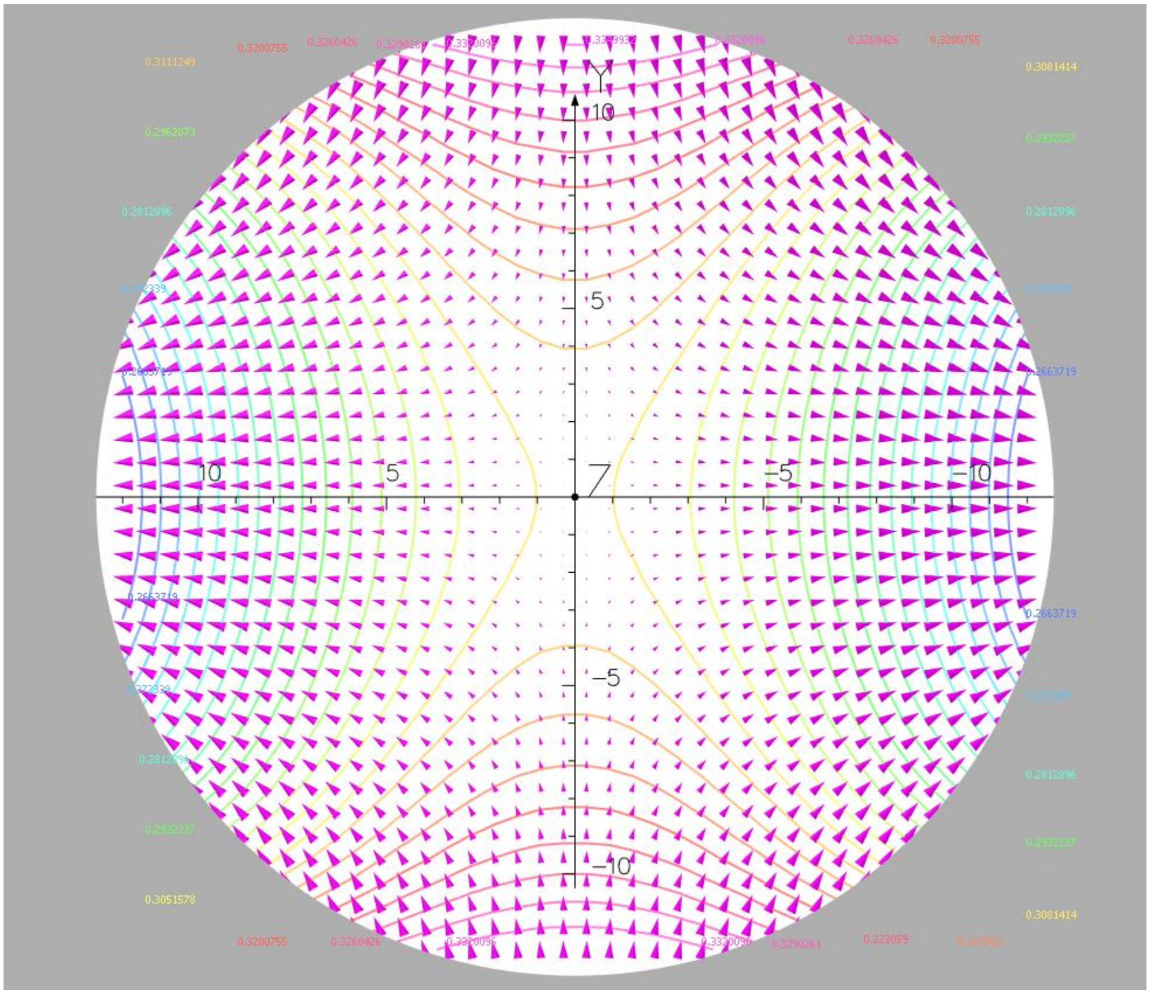

Figure 4: `Opera3D` simulation of horizontal and identical polarity parallel plate steerer with a grounded skimmer featuring a circular aperture, representing but not exactly replicating the dimensions of the ISAC/OLIS devices. **In this view, the plates are at the top and bottom of the figure, running from left to right. There are no plates on the left or right sides.** The figure is seen from the point of view of the beam, at the symmetry point between plates, from the outside of the skimmer plate, looking inward (see Fig. 3). Potentials along a surface normal to the beam propagation axis, midway between the steerer plate and skimmer electrode are shown as lines. The transverse electric field vectors are shown as purple arrows. **Warping of the field line paths to ground introduced by the circular aperture, coupled with the like-polarity of both plates, causes a quadrupole field.**

5 Index of Emittances at 8.16 keV Energy (MCIS Out)

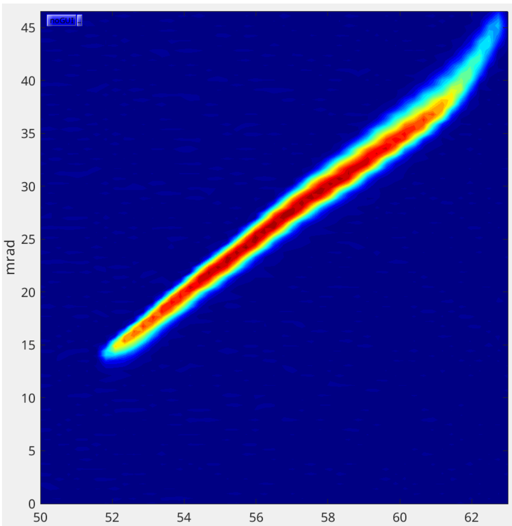

Figure 5: **240221_1430ILTEMIT.txt**

Start	End	Steps	Range	Steps	Offset
50	63	51	40	101	40

Delay	Interval	Gain	MCOL3A	MCOL3B
0.050	0.2 sec	3.3 nA	19888(1mm)	21680(1mm)

2xrms[mm]	2x'rms[mrad]	r_{12}	emit-x[μm]
5.72	15.2	0.982	16.3

^{40}Ar$^+$, E=8.16 keV, **MCIS out**.

Tune: Snapshot-5945. CCB: 100V

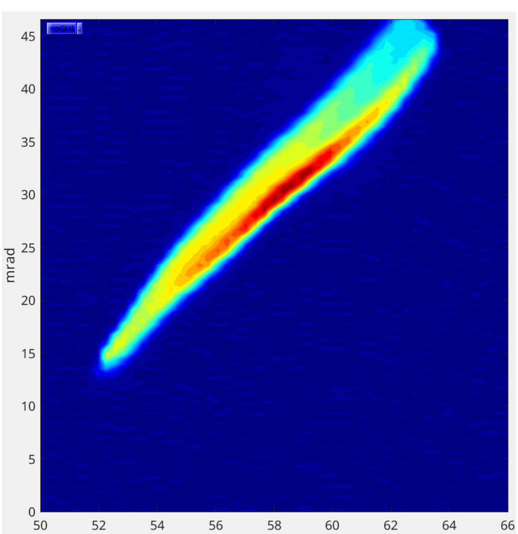

Figure 6: **240221_1507ILTEMIT.txt**

Start	End	Steps	Range	Steps	Offset
50	63	51	40	101	40

Delay	Interval	Gain	MCOL3A	MCOL3B
0.050	0.2 sec	3.3 nA	8992(5mm)	9856(5mm)

2xrms[mm]	2x'rms[mrad]	r_{12}	emit-x[μm]
5.8	15.8	0.948	29

^{40}Ar$^+$, E=8.16 keV, **MCIS out**.

Tune: Same as 5945. CCB: 100V

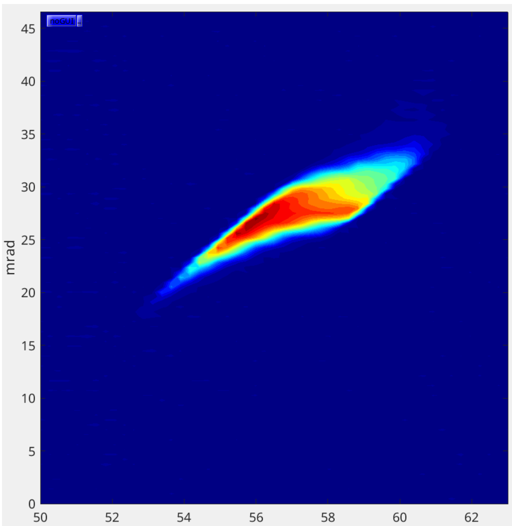

Figure 7: **240221_1418ILTEMIT.txt**

Start	End	Steps	Range	Steps	Offset
50	63	51	40	101	40

Delay	Interval	Gain	MCOL3A	MCOL3B
0.050	0.2 sec	3.3 nA	19888(1mm)	21696(1mm)

2xrms[mm]	2x'rms[mrad]	r_{12}	emit-x[μm]
3.08	5.3	0.841	8.83

$^{40}Ar^{+}$, E=8.16 keV, **MCIS out**.

Tune: Snapshot-5944. CCB: 200V

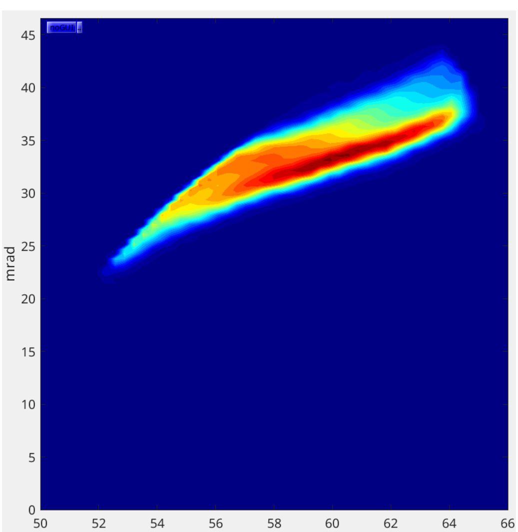

Figure 8: **240221_1513ILTEMIT.txt**

Start	End	Steps	Range	Steps	Offset
50	63	51	40	101	40

Delay	Interval	Gain	MCOL3A	MCOL3B
0.050	0.2 sec	3.3 nA	19888(1mm)	21696(1mm)

2xrms[mm]	2x'rms[mrad]	r_{12}	emit-x[μm]
5.81	7.07	0.884	19.2

$^{40}Ar^{+}$, E=8.16 keV, **MCIS out**.

Tune: Same as 5944. CCB: 200V

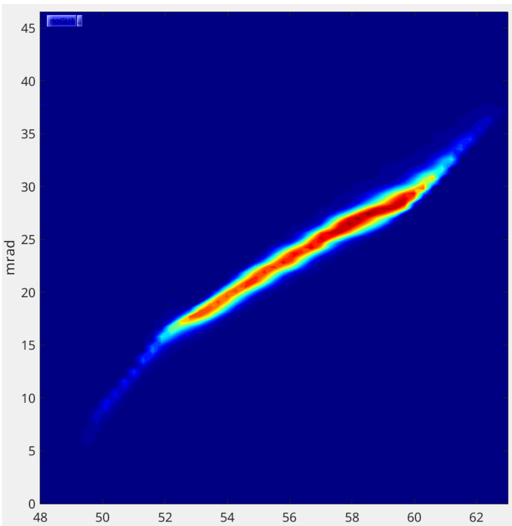

Figure 9: **240220_1544ILTEMIT.txt**

Start	End	Steps	Range	Steps	Offset
50	63	51	40	101	40

Delay	Interval	Gain	MCOL3A	MCOL3B
0.050	0.2 sec	3.3 nA	19792(1mm)	21328(1mm)

2xrms[mm]	2x'rms[mrad]	r_{12}	emit-x[μm]
5.29	9.76	0.969	12.7

^{40}Ar^{+}, E=8.16 keV, **MCIS out**.

Tune: Snapshot-5940. CCB: 300V

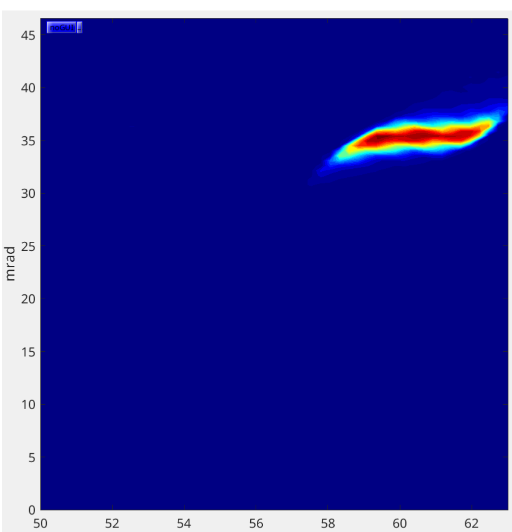

Figure 10: **240221_1444ILTEMIT.txt**

Start	End	Steps	Range	Steps	Offset
50	63	51	40	101	40

Delay	Interval	Gain	MCOL3A	MCOL3B
0.050	0.2 sec	3.3 nA	19888(1mm)	21680(1mm)

2xrms[mm]	2x'rms[mrad]	r_{12}	emit-x[μm]
2.36	2.85	0.585	5.47

^{40}Ar^{+}, E=8.16 keV, **MCIS out**.

Tune: Snapshot-5946. CCB: 400V

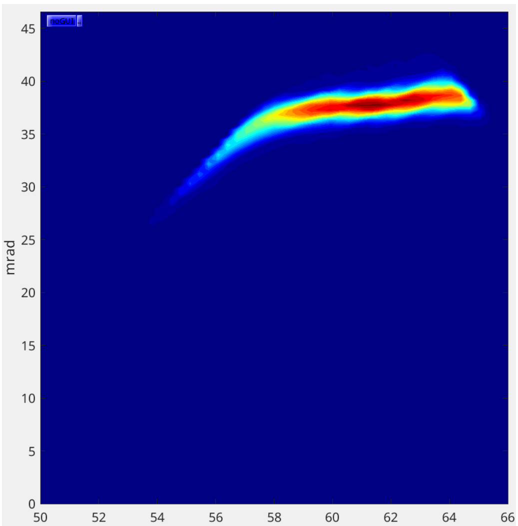

Figure 11: **240221_1500ILTEMIT.txt**

Start	End	Steps	Range	Steps	Offset
50	66	51	40	101	40

Delay	Interval	Gain	MCOL3A	MCOL3B
0.050	0.2 sec	3.3 nA	8992(5mm)	9856(5mm)

2xrms[mm]	2x'rms[mrad]	r_{12}	emit-x[μm]
4.83	3.66	0.702	12.6

^{40}Ar^{+}, E=8.16 keV, **MCIS out**.

Tune: Same as 5946. CCB: 400V

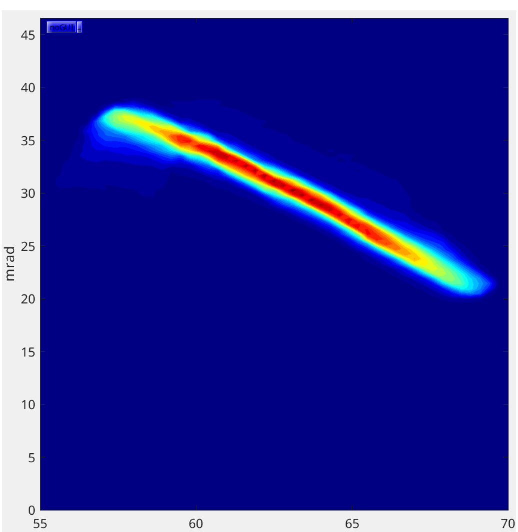

Figure 12: **240221_1546ILTEMIT.txt**

Start	End	Steps	Range	Steps	Offset
50	63	51	40	101	40

Delay	Interval	Gain	MCOL3A	MCOL3B
0.050	0.2 sec	3.3 nA	8992(5mm)	9856(5mm)

2xrms[mm]	2x'rms[mrad]	r_{12}	emit-x[μm]
6.71	9.17	-0.945	20.1

^{40}Ar^{+}, E=8.16 keV, **MCIS out**.

Tune: Snapshot-5948. CCB: 420V

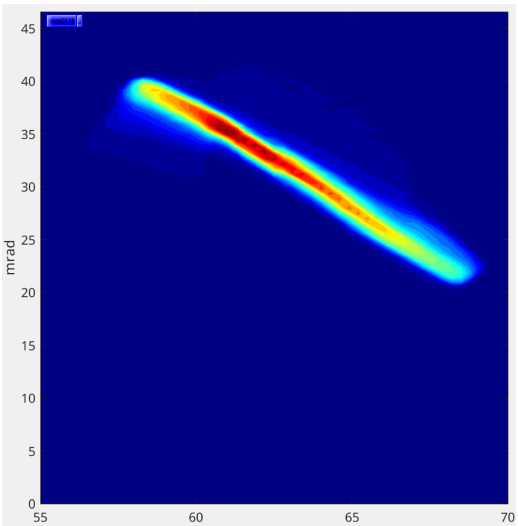

Figure 13: **240221_1537ILTEMIT.txt**

Start	End	Steps	Range	Steps	Offset
50	63	51	40	101	40

Delay	Interval	Gain	MCOL3A	MCOL3B
0.050	0.2 sec	3.3 nA	8992(5mm)	9856(5mm)

2xrms[mm]	2x'rms[mrad]	r_{12}	emit-x[μm]
6.01	10.1	-0.932	21.9

^{40}Ar^{+}, E=8.16 keV, **MCIS out**.

Tune: Snapshot-5947. CCB: 450V

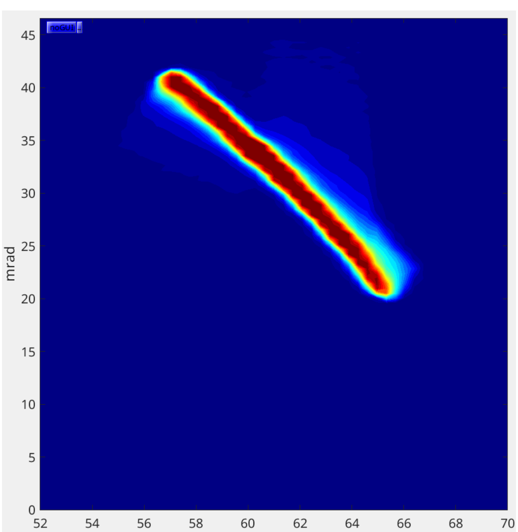

Figure 14: **240221_1036ILTEMIT.txt**

Start	End	Steps	Range	Steps	Offset
50	63	51	40	101	40

Delay	Interval	Gain	MCOL3A	MCOL3B
0.050	0.2 sec	3.3 nA	8976(5mm)	9856(5mm)

2xrms[mm]	2x'rms[mrad]	r_{12}	emit-x[μm]
5.24	11.5	-0.916	24.4

^{40}Ar^{+}, E=8.16 keV, **MCIS out**.

Tune: Snapshot-5941. CCB: 500V

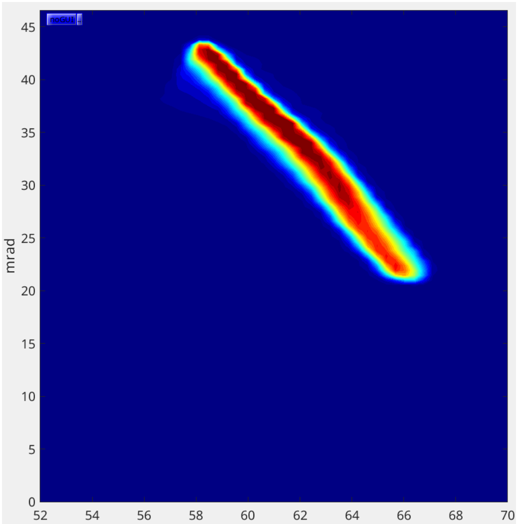

Figure 15: **240221_1049ILTEMIT.txt**

Start	End	Steps	Range	Steps	Offset
50	63	51	40	101	40

Delay	Interval	Gain	MCOL3A	MCOL3B
0.050	0.2 sec	3.3 nA	8992(5mm)	9856(5mm)

2xrms[mm]	2x'rms[mrad]	r_{12}	emit-x[μm]
4.71	12.1	-0.944	18.7

^{40}Ar^{+}, E=8.16 keV, **MCIS out**.

Tune: Snapshot-5943. CCB: 500V

6 Index of Emittances at 8.16 keV Energy (MCIS In)

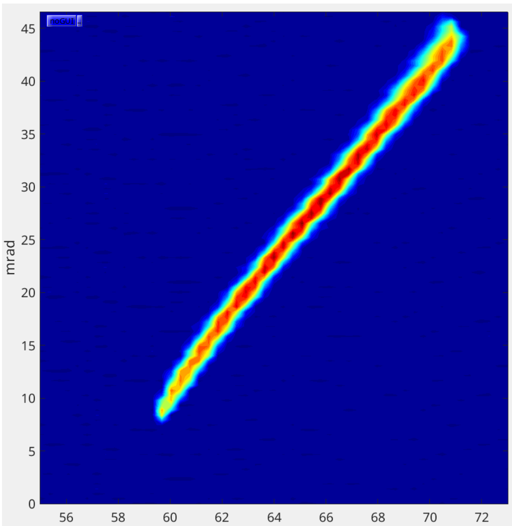

Figure 16: **240223_1445ILTEMIT.txt**

Start	End	Steps	Range	Steps	Offset
55	73	51	40	101	40

Delay	Interval	Gain	MCOL3A	MCOL3B
0.050	0.2 sec	10 nA	19712(1mm)	21680(1mm)

2xrms[mm]	2x'rms[mrad]	r_{12}	emit-x[μm]
6.55	19.9	0.986	21.4

^{40}Ar^{+}, E=8.16 keV, **MCIS in**.

Tune: E-log snapshot. CCB: 100V

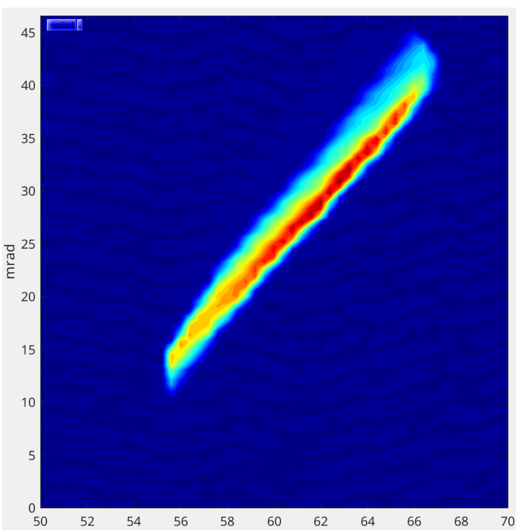

Figure 17: **240223_1049ILTEMIT.txt**

Start	End	Steps	Range	Steps	Offset
50	70	51	40	101	40

Delay	Interval	Gain	MCOL3A	MCOL3B
0.050	0.2 sec	10 nA	8992(5mm)	9856(5mm)

2xrms[mm]	2x'rms[mrad]	r_{12}	emit-x[μm]
6.18	15.8	0.97	23.9

^{40}Ar^{+}, E=8.16 keV, **MCIS in**.

Tune: E-log snapshot. CCB: 100V

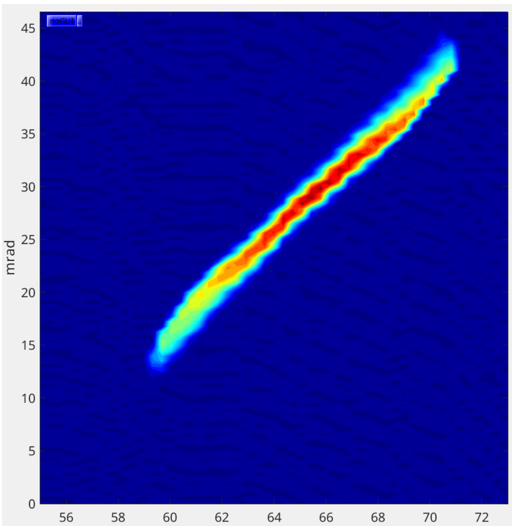

Figure 18: **240223_1435ILTEMIT.txt**

Start	End	Steps	Range	Steps	Offset
55	73	51	40	101	40

Delay	Interval	Gain	MCOL3A	MCOL3B
0.050	0.2 sec	10 nA	19712(1mm)	21680(1mm)

2xrms[mm]	2x'rms[mrad]	r_{12}	emit-x[μm]
6.32	15.0	0.993	11.3

^{40}Ar^{+}, E=8.16 keV, **MCIS in**.

Tune: E-log snapshot. CCB: 200V

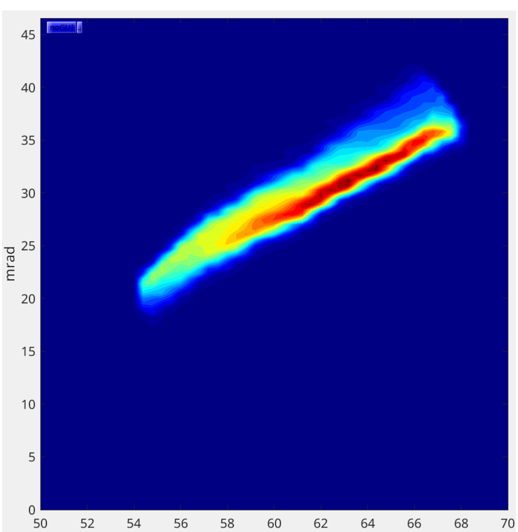

Figure 19: **240223_1004ILTEMIT.txt**

Start	End	Steps	Range	Steps	Offset
50	70	51	40	101	40

Delay	Interval	Gain	MCOL3A	MCOL3B
0.050	0.2 sec	10 nA	8992(5mm)	9856(5mm)

2xrms[mm]	2x'rms[mrad]	r_{12}	emit-x[μm]
7.14	9.12	0.92	25.5

^{40}Ar^{+}, E=8.16 keV, **MCIS in**.

Tune: E-log snapshot. CCB: 200V

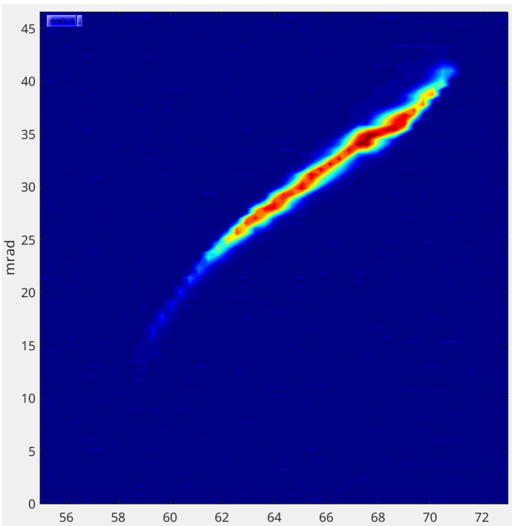

Figure 20: **240223_1343ILTEMIT.txt**

Start	End	Steps	Range	Steps	Offset
55	73	51	40	101	40

Delay	Interval	Gain	MCOL3A	MCOL3B
0.050	0.2 sec	10 nA	19712(1mm)	21680(1mm)

2xrms[mm]	2x'rms[mrad]	r_{12}	emit-x[μm]
5.22	9.78	0.979	10.8

^{40}Ar^{+}, E=8.16 keV, **MCIS in**.

Tune: E-log snapshot. CCB: 300V

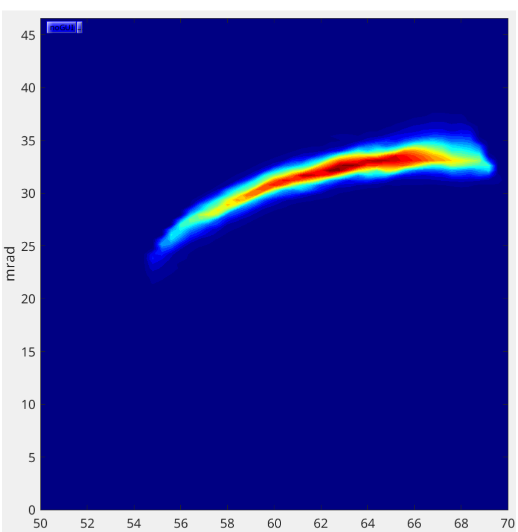

Figure 21: **240223_1026ILTEMIT.txt**

Start	End	Steps	Range	Steps	Offset
50	70	51	40	101	40

Delay	Interval	Gain	MCOL3A	MCOL3B
0.050	0.2 sec	10 nA	8992(5mm)	9856(5mm)

2xrms[mm]	2x'rms[mrad]	r_{12}	emit-x[μm]
7.39	4.77	0.838	19.2

^{40}Ar^{+}, E=8.16 keV, **MCIS in**.

Tune: E-log snapshot. CCB: 300V

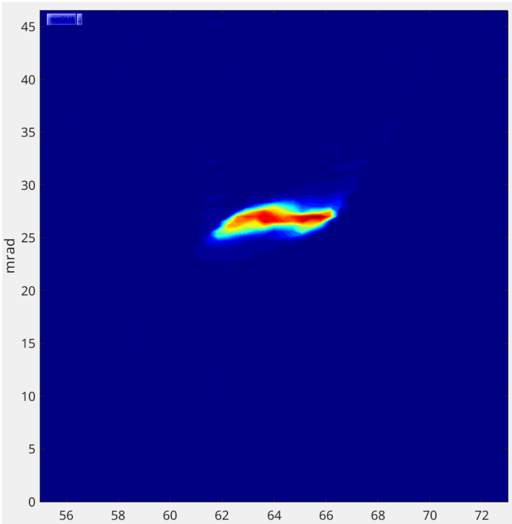

Figure 22: **240223_1310ILTEMIT.txt**

Start	End	Steps	Range	Steps	Offset
55	73	51	40	101	40

Delay	Interval	Gain	MCOL3A	MCOL3B
0.050	0.2 sec	10 nA	19712(1mm)	21680(1mm)

2xrms[mm]	2x'rms[mrad]	r_{12}	emit-x[μm]
2.51	1.92	0.451	4.48

$^{40}Ar^{+}$, E=8.16 keV, **MCIS in**.

Tune: E-log snapshot. CCB: 350V

Note: In Figure 22, beam has been mismatched by steerer lensing at the OLIS 1mm collimators, causing clipping of the beam distribution.

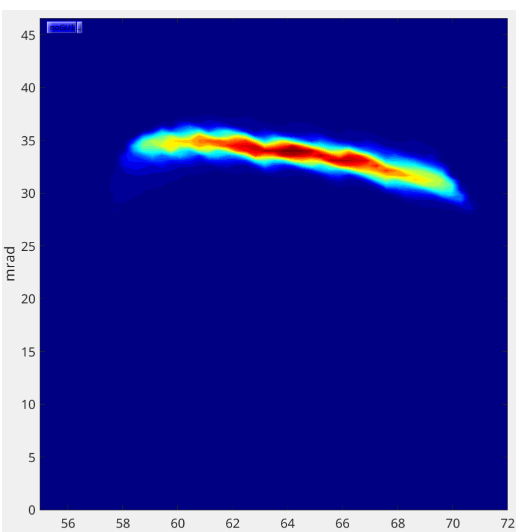

Figure 23: **240223_1043ILTEMIT.txt**

Start	End	Steps	Range	Steps	Offset
50	70	51	40	101	40

Delay	Interval	Gain	MCOL3A	MCOL3B
0.050	0.2 sec	10 nA	8992(5mm)	9856(5mm)

2xrms[mm]	2x'rms[mrad]	r_{12}	emit-x[μm]
6.43	3.25	-0.616	16.5

$^{40}Ar^{+}$, E=8.16 keV, **MCIS in**.

Tune: E-log snapshot. CCB: 350V

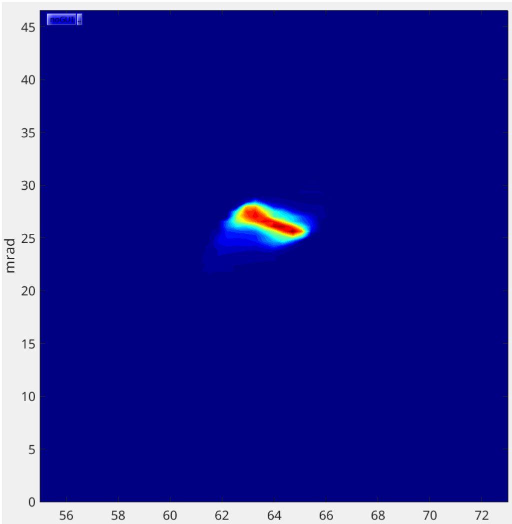

Figure 24: **240223_1243ILTEMIT.txt**

Start	End	Steps	Range	Steps	Offset
55	73	51	40	101	40

Delay	Interval	Gain	MCOL3A	MCOL3B
0.050	0.2 sec	10 nA	19712(1mm)	21680(1mm)

2xrms[mm]	2x'rms[mrad]	r_{12}	emit-x[μm]
1.79	2.75	0.0252	4.93

^{40}Ar$^+$, E=8.16 keV, **MCIS in**.

Tune: E-log snapshot. CCB: 400V

Note: In Figure 24, beam has been mismatched by steerer lensing at the OLIS 1mm collimators, causing clipping of the beam distribution.

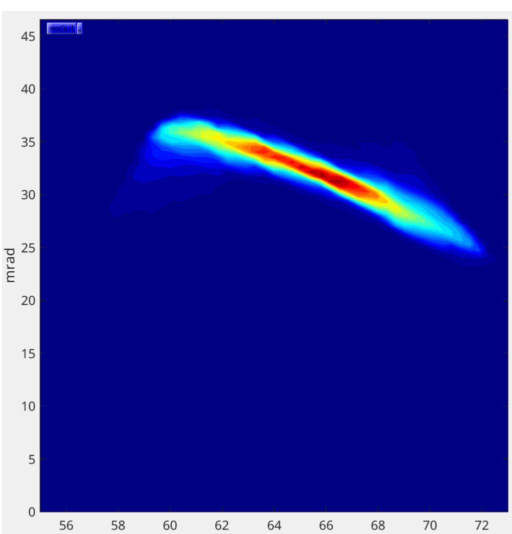

Figure 25: **240223_1059ILTEMIT.txt**

Start	End	Steps	Range	Steps	Offset
55	73	51	40	101	40

Delay	Interval	Gain	MCOL3A	MCOL3B
0.050	0.2 sec	10 nA	8992(5mm)	9856(5mm)

2xrms[mm]	2x'rms[mrad]	r_{12}	emit-x[μm]
6.6	5.46	-0.924	13.8

^{40}Ar$^+$, E=8.16 keV, **MCIS in**.

Tune: E-log snapshot. CCB: 400V

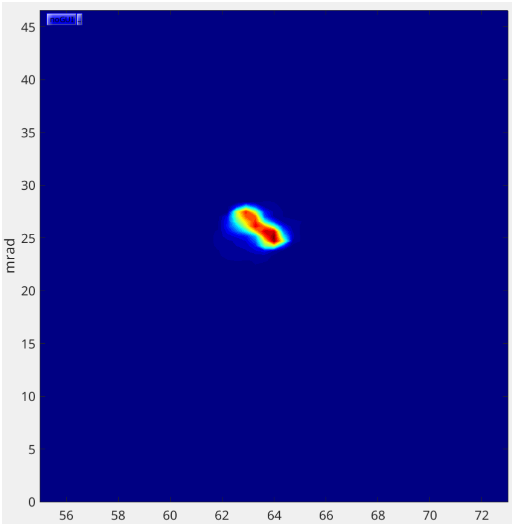

Figure 26: **240223_1223ILTEMIT.txt**

Start	End	Steps	Range	Steps	Offset
55	73	51	40	101	40

Delay	Interval	Gain	MCOL3A	MCOL3B
0.050	0.2 sec	10 nA	19712(1mm)	21680(1mm)

2xrms[mm]	2x'rms[mrad]	r_{12}	emit-x[μm]
1.21	2.28	-0.314	2.7

^{40}Ar^{+}, E=8.16 keV, **MCIS in**.

Tune: E-log snapshot. CCB: 420V

Note: In Figure 26, beam has been mismatched by steerer lensing at the OLIS 1mm collimators, causing clipping of the beam distribution.

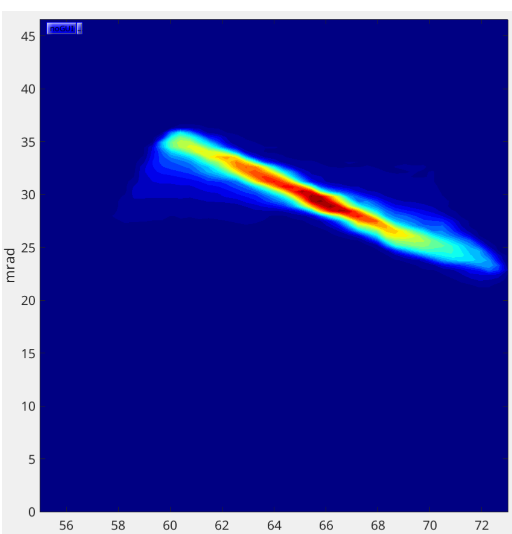

Figure 27: **240223_1109ILTEMIT.txt**

Start	End	Steps	Range	Steps	Offset
55	73	51	40	101	40

Delay	Interval	Gain	MCOL3A	MCOL3B
0.050	0.2 sec	10 nA	8992(5mm)	9856(5mm)

2xrms[mm]	2x'rms[mrad]	r_{12}	emit-x[μm]
6.94	5.9	-0.94	14.0

^{40}Ar^{+}, E=8.16 keV, **MCIS in**.

Tune: E-log snapshot. CCB: 420V

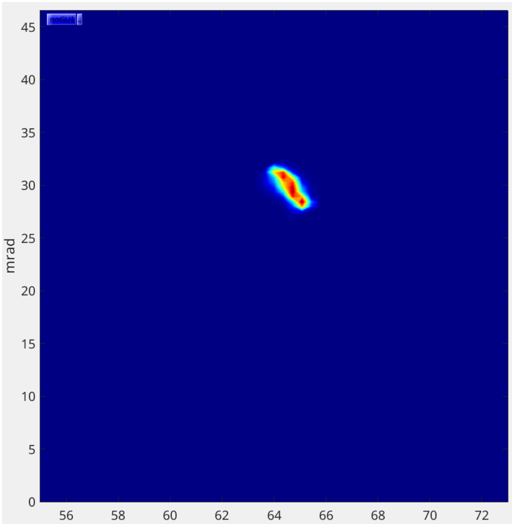

Figure 28: **240223_1159ILTEMIT.txt**

Start	End	Steps	Range	Steps	Offset
55	73	51	40	101	40

Delay	Interval	Gain	MCOL3A	MCOL3B
0.050	0.2 sec	10 nA	19712(1mm)	21680(1mm)

2xrms[mm]	2x'rms[mrad]	r_{12}	emit-x[μm]
0.919	2.36	-0.389	2.0

^{40}Ar^{+}, E=8.16 keV, **MCIS in**.

Tune: E-log snapshot. CCB: 450V

Note: In Figure 28, beam has been mismatched by steerer lensing at the OLIS 1mm collimators, causing clipping of the beam distribution.

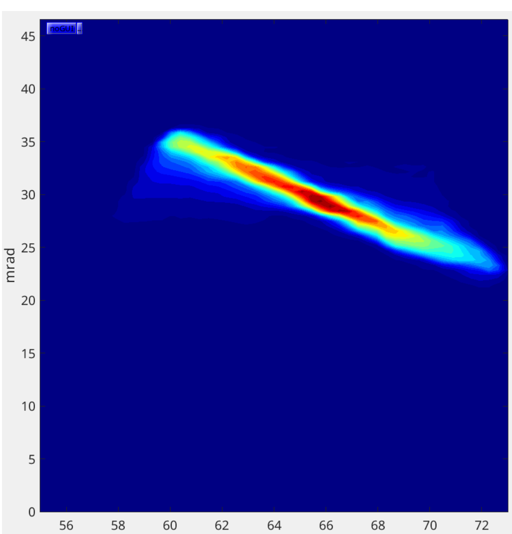

Figure 29: **240223_1118ILTEMIT.txt**

Start	End	Steps	Range	Steps	Offset
55	73	51	40	101	40

Delay	Interval	Gain	MCOL3A	MCOL3B
0.050	0.2 sec	10 nA	8992(5mm)	9856(5mm)

2xrms[mm]	2x'rms[mrad]	r_{12}	emit-x[μm]
6.94	5.9	-0.94	14.0

^{40}Ar^{+}, E=8.16 keV, **MCIS in**.

Tune: E-log snapshot. CCB: 450V

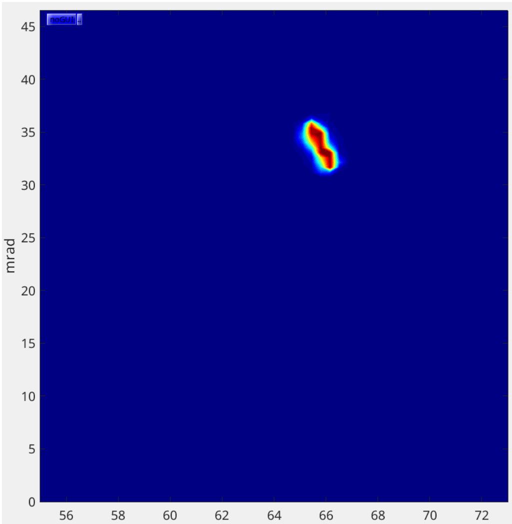

Figure 30: **240223_1142ILTEMIT.txt**

Start	End	Steps	Range	Steps	Offset
55	73	51	40	101	40

Delay	Interval	Gain	MCOL3A	MCOL3B
0.050	0.2 sec	10 nA	19712(1mm)	21680(1mm)

2xrms[mm]	2x'rms[mrad]	r_{12}	emit-x[μm]
0.777	2.95	-0.562	1.9

^{40}Ar^{+}, E=8.16 keV, **MCIS in**.

Tune: E-log snapshot. CCB: 500V

Note: In Figure 30, beam has been mismatched by steerer lensing at the OLIS 1mm collimators, causing clipping of the beam distribution.

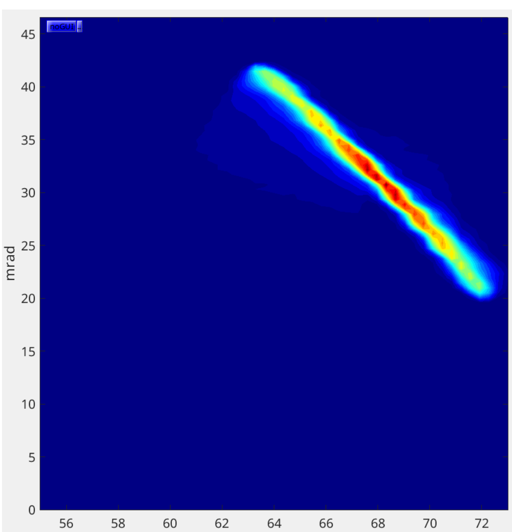

Figure 31: **240223_1127ILTEMIT.txt**

Start	End	Steps	Range	Steps	Offset
55	73	51	40	101	40

Delay	Interval	Gain	MCOL3A	MCOL3B
0.050	0.2 sec	10 nA	8992(5mm)	9856(5mm)

2xrms[mm]	2x'rms[mrad]	r_{12}	emit-x[μm]
5.23	11.0	-0.985	10.1

^{40}Ar^{+}, E=8.16 keV, **MCIS in**.

Tune: E-log snapshot. CCB: 500V

7 Conclusion

This report has presented emittance based evidence of steerer lensing at the ISAC-OLIS facility, both with and without the MCIS/supernanogan installed in the OLIS high voltage terminal. Focal effects arising from corrective steerers, which is an energy dependent effect, will affect all OLIS beams to varying degrees.

As a result of the findings presented in this report, work on the full characterization of the focal properties of the ISAC electrostatic steerers has been initiated and will be reported in future work. This shall lead to a corrective prescription to the presented pathologies, intended to both improve operational simplicity for OLIS tuning and lead to a sustained reduction in tuning times, by enabling accurate parallel modelling of the source and beamlines.

8 Acknowledgements

Thanks to R. Baartman for useful discussions and valuable advice and insight into the OLIS system, in addition to historical data on the I1 issue. T. Planche is also thanked for support regarding Opera simulations and knowledge on the issue of parallel plate steerers coupled with round-aperture grounding skimmers. O. Kester is sincerely thanked for supporting the nascent machine development effort at ISAC, which made these findings possible. Thanks to F. Ames for useful discussions and insight into source physics and OLIS. Thanks to RIB Operators for assistance during beam measurements, invaluable for this report and its conclusions. Thanks to C. Charles, B. Minato and M. Lovera for OLIS preparation including installation of the MCIS cart.

References

[1] K Jayamanna, I Aguilar, I Bylinskii, G Cojocaru, RL Dube, R Laplante, D Louie, M Lovera, B Minato, M Mouat, et al. A 20 mA H-minus Ion Source with ACCEL-ACCEL-DECEL Extraction System at TRIUMF.

[2] Joseph Adegun. personal communication.

[3] Olivier Shelbaya. Anomalous Operational OLIS Tunes. Technical Report TRI-BN-19-20, TRIUMF, 2019.

[4] Olivier Shelbaya. OLIS to RFQ Beam Transport and Acceleration in TRANSOPTR. Technical Report TRI-BN-20-13, TRIUMF, 2020.

[5] Reinard Becker and WB Herrmannsfeldt. IGUN - A program for the simulation of positive ion extraction including magnetic fields. *Review of scientific instruments*, 63(4):2756–2758, 1992.

[6] Olivier Shelbaya. Sequential Tune Optimization with TRANSOPTR. Technical Report TRI-BN-20-14, TRIUMF, 2020.

[7] Olivier Shelbaya. Model Coupled Accelerator Tuning (PhD thesis). Technical Report TRI-BN-23-04, TRIUMF, UVic Dept. of Physics & Astronomy, 2023. https://dspace.library.uvic.ca/handle/1828/14804.

[8] Olivier Shelbaya. Report On OLIS Quadrupoles 5 and 7 . Technical Report TRI-BN-22-12, TRIUMF, 2022.

[9] Olivier Shelbaya and Richard Baartman. Langevin-Like DTL Triplet BI Fits and Analysis of Transverse DTL Tuning Difficulties. Technical Report TRI-BN-19-18, TRIUMF, 2019.

[10] JA Maloney, R Baartman, T Planche, and S Saminathan. Electrostatic potential map modelling with cosy infinity. *Nuclear Instruments and Methods in Physics Research Section B: Beam Interactions with Materials and Atoms*, 376:171–174, 2016.

[11] I Bylinskii, R Baartman, K Jayamanna, T Planche, and YN Rao. Recent improvements in beam delivery with the triumf's 500 mev cyclotron. *Proceedings of Cyclotrons2016, Zurich, Switzerland*, pages 133–136, 2017.